Direct-Write Assembly of Microperiodic Silk Fibroin Scaffolds for Tissue Engineering Applications**

By *Sourabh Ghosh, Sara T. Parker, Xianyan Wang, David L. Kaplan,* and *Jennifer A. Lewis**

Three–dimensional, microperiodic scaffolds of regenerated silk fibroin have been fabricated for tissue engineering by direct ink writing. The ink, which consisted of silk fibroin solution from the *Bombyx mori* silkworm, was deposited in a layer-by-layer fashion through a fine nozzle to produce a 3D array of silk fibers of diameter 5 μm. The extruded fibers crystallized when deposited into a methanol-rich reservoir, retaining a pore structure necessary for media transport. The rheological properties of the silk fibroin solutions were investigated and the crystallized silk fibers were characterized for structure and mechanical properties by infrared spectroscopy and nanoindentation, respectively. The scaffolds supported human bone marrow-derived mesenchymal stem cell (hMSC) adhesion, and growth. Cells cultured under chondrogenic conditions on these scaffolds supported enhanced chondrogenic differentiation based on increased glucosaminoglycan production compared to standard pellet culture. Our results suggest that 3D silk fibroin scaffolds may find potential application as tissue engineering constructs due to the precise control of their scaffold architecture and their biocompatibility.

1. Introduction

Tissue engineering has progressed toward the goal of regeneration of tissue constructs to restore or replace lost morphological and functional features of diseased or damaged organs. Emerging trends in the field also include establishing in vitro human disease model systems to gain fundamental insight into pathological conditions,[1,2] and simulating complex processes during tissue development in vitro to gather detailed insight into developmental biology.[3] The goal is to exploit this insight for improved tissue regeneration strategies. To achieve these objectives, there is a need to develop tissue composite systems to recapitulate the complex three-dimensional (3D) morphology, architecture, and microenvironments of the target tissue or pathological condition. These constructs also need to consider biomechanical forces and hydrodynamic fluid transport to accommodate the requirements in the targeted tissues.

Conventional two-dimensional (2D) in vitro cell culture systems provide a convenient and rapid platform for biochemical analysis, but lack the above nuances of 3D tissues, including the transport and complexity related to cell signaling and responses. Cells respond to 3D architectures in ways that can not be replicated in conventional monolayer cell culture, especially with respect to complex local signals from homotypic or heterotypic cell adhesion, mechanical forces and biochemical signals.[4,5] The ability to fabricate 3D scaffolds specifically for targeted tissue microenvironments would provide improved options to regulate cell adhesion, cell proliferation, expression of a specific phenotypes, and influence the deposition and organization of new extracellular matrix.

The regeneration of a tissue is a coordinated constellation of spatial and temporal signals originating from extracellular microenvironments. These signals come from biomaterial scaffold surface chemistry, mechanical stiffness and surface topography, as well as from cell–cell signaling and soluble factors added in culture media. For example, mesenchymal stem cells (MSC) undergo differentiation to chondrocytes when they are exposed to environmental cues in 3D culture in the presence of certain factors (e.g., insulin, dexamethasone, an isoform of transforming growth factor (TGF) family).[6–8] At the macroscale level, scaffold architecture facilitates coordination of multicellular processes typical of 3D tissue microenvironments.

Previous efforts to fabricate 3D spatiotemporal tissue organization have focused on the modulation of nonadhesive properties of culture substrates,[4,9] such as with agarose or poly-hydroxyethyl methacrylate coatings, or by using traditional scaffold fabrication techniques, such as solvent casting, temperature-induced phase separation, nonwoven fiber meshes,[10] particle-leaching techniques,[11] or gas foaming.[12] These approaches provide porous interconnected polymer

[*] Prof. D. L. Kaplan, Dr. S. Ghosh, Dr. X. Wang
Department of Biomedical Engineering, Tufts University
Boston, MA 02155 (USA)
E-mail: david.kaplan@tufts.edu
Prof. J. A. Lewis, S. T. Parker
Department of Materials Science and Engineering
Urbana, IL 61801 (USA)
E-mail: jalewis@uiuc.edu

© 2008 WILEY-VCH Verlag GmbH & Co. KGaA, Weinheim

WILEY InterScience®
DISCOVER SOMETHING GREAT

architectures; however the control over scaffold features are process driven, as opposed to specified by design. Therefore, it is difficult to tune the micro- and macroscale architectural features of scaffolds using these methods. Rapid prototyping-based manufacturing techniques can be used to generate scaffolds having precisely controlled micro- and nanoscale architectures and highly interconnected pores using computer aided design/machining approaches. For example, stereolithography, selective laser sintering, and three-dimensional printing,[13–19] have been employed to deposit thermoplastic polymers in layer-by-layer approaches that result in 3D fibrous architectures with fiber diameters that range from 150–400 μm. These scaffolds are important in the field of tissue engineering, as they offer enhanced mass transfer of nutrients, oxygen and metabolic wastes due to the interconnected porous architecture compared to conventionally fabricated particle-leached porous scaffolds. However, due to the large fiber diameters, cells tend to respond as if they are on a 2D surface, leading to a nonphysiological asymmetrical gathering of adhesion receptors, and thus less relevant physiological outcomes.[20]

The term 'direct-write' describes assembly methods that employ a computer-controlled translation stage that moves a pattern-generating device (e.g., ink deposition nozzle or laser writing optics) in a layer-by-layer sequence, to form materials with controlled architectures and composition in complex 3D structures. We have recently shown that this simple, flexible, and inexpensive approach can be utilized to create 3D structures from inks composed of polyelectrolyte complexes or colloidal gels.[21,22] Fabrication of micropatterened architectures by this technique offers the potential to provide control of cell location, orientation, alignment, migration and aggregation on the basis of a wide range of architectural cues. We therefore aim to extend direct-write assembly to a more tissue-relevant scaffold biomaterial in order to investigate cell-based responses on such architectures. Silk fibroin protein was selected as the 'ink' due to its superb biocompatibility, robust mechanical properties, including high mechanical modulus and toughness, relatively slow proteolytic biodegradation, the ability to utilize aqueous solutions, and the ability to control structure. This combination of features is particularly unique for degradable biocompatible polymers and prompted the use of this protein polymer in the present studies. Further, since silk is naturally 'spun' from aqueous solution to form strong fibers, the present approach in part mimics this process. In addition, this protein has been extensively used in the field of regenerative medicine for surgical needs, in drug delivery,[23] and as scaffolds for tissue engineering.[11,24–28]

Here, we describe the formation of 3D microperiodic scaffolds by direct writing of silk fibroin from aqueous solutions of regenerated *Bombyx mori* silk. A number of parameters, such as ink composition, nozzle size, deposition speed, coagulant bath composition, and scaffold pitch, were assessed. Importantly, these scaffolds contained feature sizes that were significantly smaller than those produced by other rapid prototyping techniques.[14–19] Initial investigations of the use of

these direct-write scaffolds on human bone marrow-derived mesenchymal stem cells (hMSCs) was also assessed with a focus on chondrogenic differentiation. The scaffolds supported both cell adhesion and growth as well as enhanced chondrogenic differentiation based on increased glucosaminoglycan production compared to standard pellet culture. The ability to produce microfabricated 3D silk architectures by direct ink writing avoids the harsh conditions of temperature or solvents thereby opening new avenues for incorporating additional bioactive components in the future, as shown with gel and electrospun nanofibrous silk systems.[29,31]

2. Results and Discussion

Silk fibroin was deposited through a microcapillary nozzle mounted onto a three-axis, computer-controlled stage into methanol-rich reservoir, such that the deposited fibers underwent rapid solidification by inducing crystallization (Fig. 1a). The morphology of the silk filaments was examined by scanning electron microscopy (SEM) and representative images of the complex 3D patterns fabricated through the direct writing of concentrated silk fibroin solution are shown in Figure 1b–c. Scaffolds consisted of a 3D microperiodic array of fibers approximately 5 μm in diameter that are much finer than those produced by other rapid prototyping methods, where fiber diameters ranged from 150–400 μm.[12,16] Their center-to-center spacing in the x–y plane was maintained at 100 μm to create a large pore geometry for cell growth and aggregation. By using a concentrated 28–30 wt% silk fibroin solution as the ink, dimensional shrinkage in the scaffolds was minimized. Surface morphology of a single printed fiber is shown in Figure 1d. The surface morphology is rougher than that observed for structures produced from polyelectrolyte complexes,[22] yet smoother than electrospun regenerated silk fibers treated with methanol.[30] In the latter case, there is likely pronounced phase separation of PEO and silk fibroin in the electrospun fibers.

The silk ink flows easily through a 5 μm nozzle and its fiber morphology is maintained upon extrusion into the methanol-rich reservoir, even as it fuses with the underlying filaments. It is well known that the addition of methanol, a poor solvent, to regenerated silk fibroin induces aggregation (dehydration), which drives the structural transition from random coil to β-sheet.[24,25] By triggering this structural transition *in situ* during the printing process, the structural integrity of the as-patterned silk scaffolds is retained. Direct-write assembly enables the fabrication of complex architectures for tissue engineering in the form of both 3D microperiodic lattices and radial arrays. (Fig. 1).

The silk fibroin solutions exhibited a pronounced shear rate dependence on viscosity at lower concentrations (<19 wt%). However, above this critical concentration, they behaved much like a Newtonian fluid with little dependence on shear rate over the range probed (Fig. 2a). The observed shear thinning
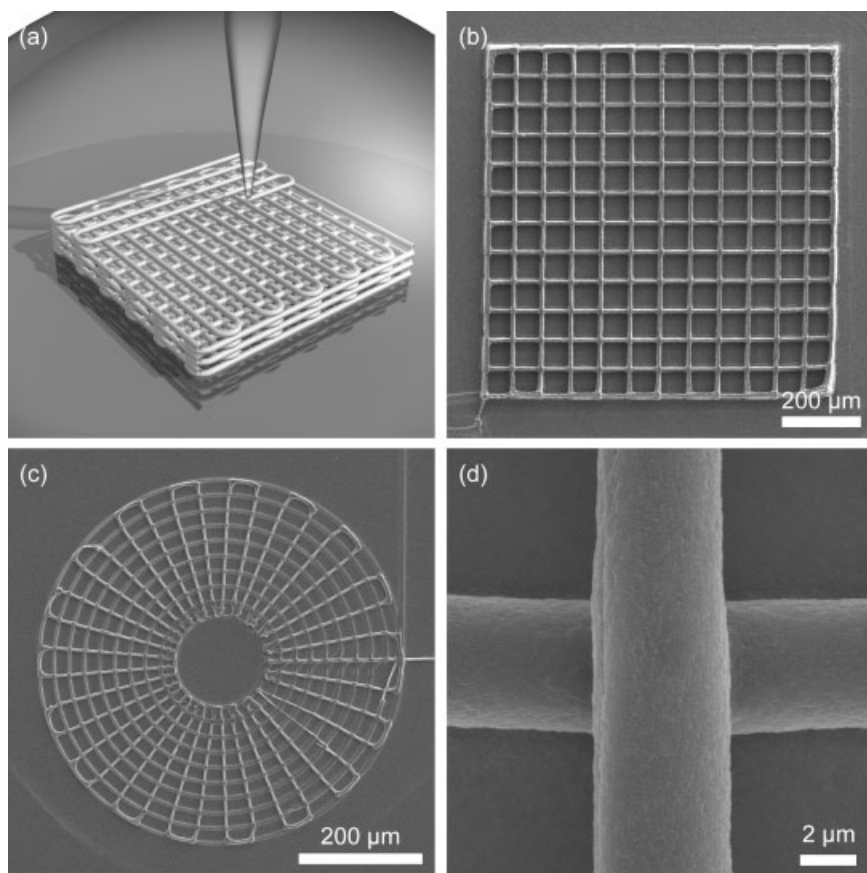
Figure 1. a) Schematic illustration of 3D direct ink writing of silk fibroin in liquid reservoir. Representative 3D structures of b) square lattice and c) circular web. d) Magnified image of direct write silk fiber.

To further investigate the rheological properties of the optimal silk fibroin solution for direct-write assembly, the storage modulus (G') and loss modulus (G'') were determined (Fig. 2b). Under oscillation at a frequency of 1 Hz, a plateau elastic modulus (G') of ~1.2 Pa and a yield stress of ~13 Pa were measured for the 29 wt% silk fibroin solution. Importantly, the 29 wt% silk solution remained liquid-like at 1 Hz, as shown by the viscous modulus (G'') remaining higher than the elastic modulus (G') for all shear stresses in the experimental range, thereby facilitating its flow through fine deposition nozzles.

Fourier Transform Infrared Spectroscopy (FTIR) was used to confirm that the printed silk protein fibers had transformed to the expected β-sheet conformation. The transmittance data for a dried film of untreated silk and for the fibers printed by direct ink writing in a methanol reservoir are shown in Figure 3. For the untreated silk sample, the absorption bands at 1660, 1540, and 1240 cm^{-1} are characteristic of random coil and correspond to the amide I, amide II, and amide III bands, respectively.[35–37] For the silk fibers printed in a methanol-rich reservoir, the spectrum revealed that these absorption bands shifted to 1624, 1516, and 1265 cm^{-1}, confirming the β-sheet structure.[37]

behavior likely reflects the formation of aggregates in solution due to hydrophobic/hydrophilic interactions.[32] Silk fibroin is an amphiphilic block co-polymer with the molecular mass of the dominant high molecular weight protein of ~390 KDa.[33] The heavy chain is composed of 12 repetitive domains, whose typical compositions are clusters of oligopeptides Gly-Ala-Gly-Ala-Gly-Ser, (Gly-Ala)n-Gly-Tyr and (Gly-Ala)n-Gly-Ala (n = 1–8), separated by 11 small amorphous regions, or spacers) consisting of more hydrophilic peptides. The dominating hydrophobic peptide repeats self-organize into the β-sheet structures, mediated by hydrophobic hydration.[34] As shear rate increases, these molecules tend to become aligned and the frictional resistance between adjacent layers of the laminar fluid decrease, resulting in shear thinning. Chain mobility is suppressed in silk fibroin solution of higher concentrations, which may hinder their ability to self-organize into an aggregated structure. The low shear viscosity of the most concentrated silk fibroin solution (29 wt%) was ~2.9 Pa, which is similar to the viscosity of synthetic polyelectrolyte complexes initially developed for direct ink writing at the microscale.[22] Thus, this ink composition was deemed optimal for scaffold printing.
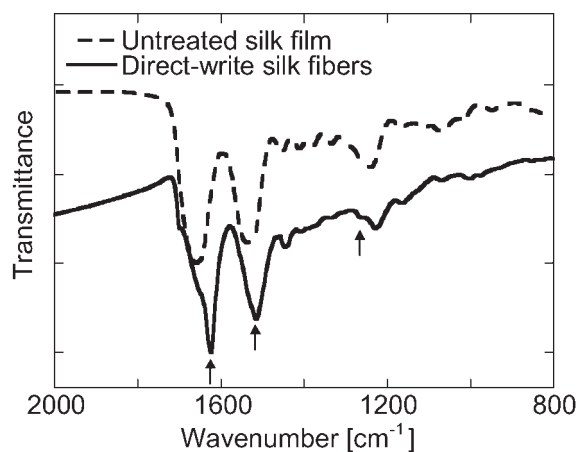
The mechanical properties of these 3D scaffolds are dependent on both their architecture and composition. Nanoindentation was carried out using atomic force microscopy (AFM) to determine their mechanical properties (Fig. 4).[38,39] The load–displacement curves for a direct-write scaffold composed of three layers of deposited fibers were compared with a scaffold of a similar thickness prepared from silk fibroin using a salt leaching technique.[14,25] The elastic modulus of direct-write scaffolds having three fiber layers (5.64 ± 1.36) GPa was slightly lower than the salt-leached porous scaffolds (8.44 ± 1.37) GPa. Such differences likely arise due to their architectural variations, that is, the direct-write technique yields periodic structures, whereas the salt-leaching method produces scaffolds with a highly irregular porous network.

To determine cell compatibility and responses on the direct-write silk scaffolds, hMSCs were cultured in chondrogenic media. Cell morphology can be used to assess growth and differentiation through mechanotransduction related to cytoskeletal signaling and remodeling, with actin microfilaments as the major structural element to consider. In vivo, during mesenchymal condensation stages of embryonic
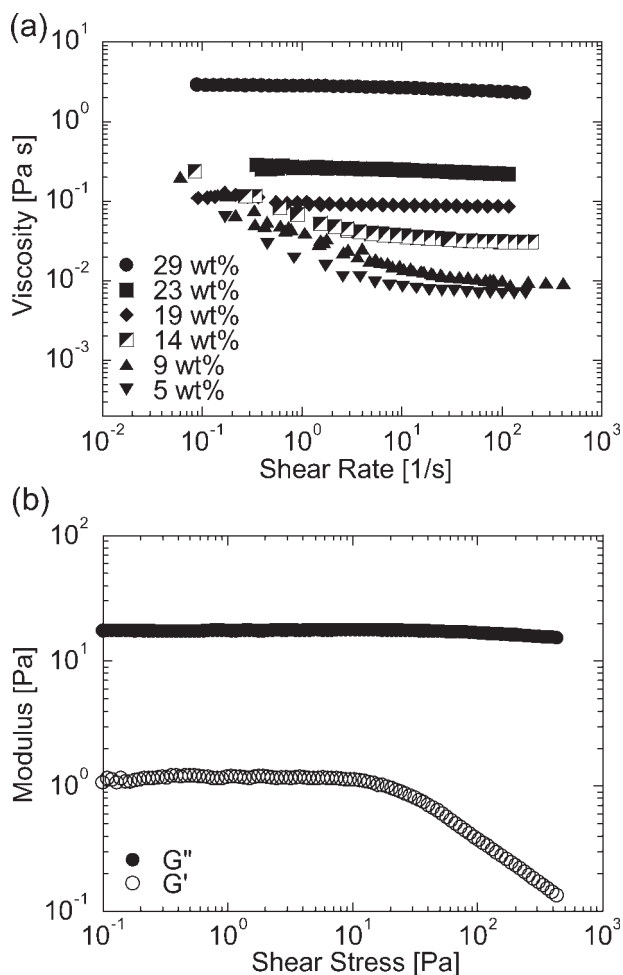
Figure 2. a) Log–log plot of viscosity as a function of shear rate for silk fibroin solutions with varying concentrations from 5–29 wt%. b) Log–log plot of shear elastic (G') and viscous (G″) moduli as a function of shear rate for 29 wt% silk fibroin ink.

Figure 3. Normalized FTIR transmittance spectra for an untreated silk fibroin film and for silk fibroin fibers deposited by direct ink writing. The arrows indicate the absorption bands at 1624, 1516, and 1265 cm^{-1}, which are characteristic of β-sheet structure.

disorganized fashion at the cortex of the oval-shaped cells was indicative of chondrogenic differentiation.[47]

The results also indicate that cells cultured on the direct-write scaffolds in control medium alone, without providing the remaining necessary soluble factors for differentiation, remained in the undifferentiated state, based on glucosaminoglycan (GAG) production. GAG, the major component of cartilage extracellular matrix, was quantified using dimethylmethylene blue (DMMB). hMSCs cultured in pellet form were used as a 'gold standard' control to determine extent of chondrogenesis.[48] After two to three weeks in culture under chondrogenic conditions, the cells adhered to the direct-write scaffold produced significantly higher amounts of GAG per DNA compared to both the controls (without chondrogenic soluble factors and to the chondrogenic pellet cultures). (Figure 6)
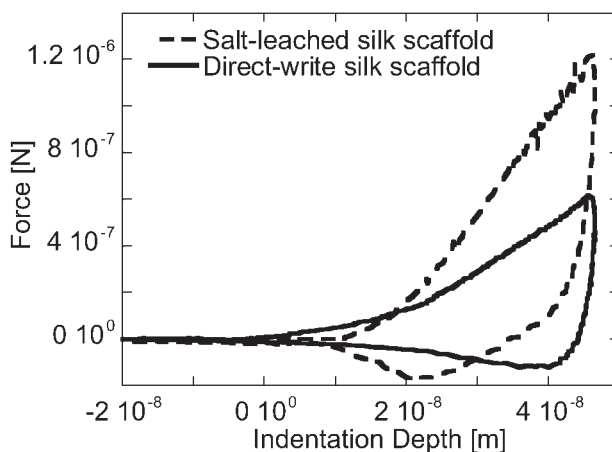
development of cartilage, cell shape changes from a fibroblastic spread morphology to a rounded morphology, with associated modulation of actin microfilament networks to a punctuated structure localized at the peripheral cortex of the differentiated cells.[40–43] In vitro, actin-disrupting compounds, such as cytochalasin D induce chondrogenesis in bone marrow derived stem cells[44–45] and embryonic mesenchymal cells.[46] Focal adhesion sites exist where mechanical stress is converted to biochemical signals in the cell, mediated by vinculin as anchoring sites of actin stress fibers to the plasma membrane integrin receptors to stabilize cell shape. Expression of vinculin is a reliable indicator of cell adhesion/spreading, loss of anchorage dependence and aggregation.[47] After 1 day on the direct-write silk scaffolds, the hMSCs assumed a spread morphology, with expression of actin stress fibers, while after two to three weeks of culture cell/cell-aggregates were observed throughout the scaffolds (Figure 5). Short punctate actin staining scattered in the cytoplasm and accumulated in a
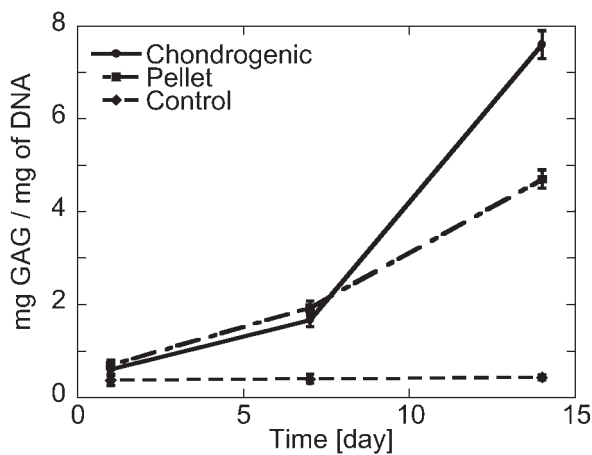

Figure 4. Loading and unloading curves of salt-leached and direct-write silk scaffolds measured by AFM naninindentation. The curves have been averaged over 6 measurements.
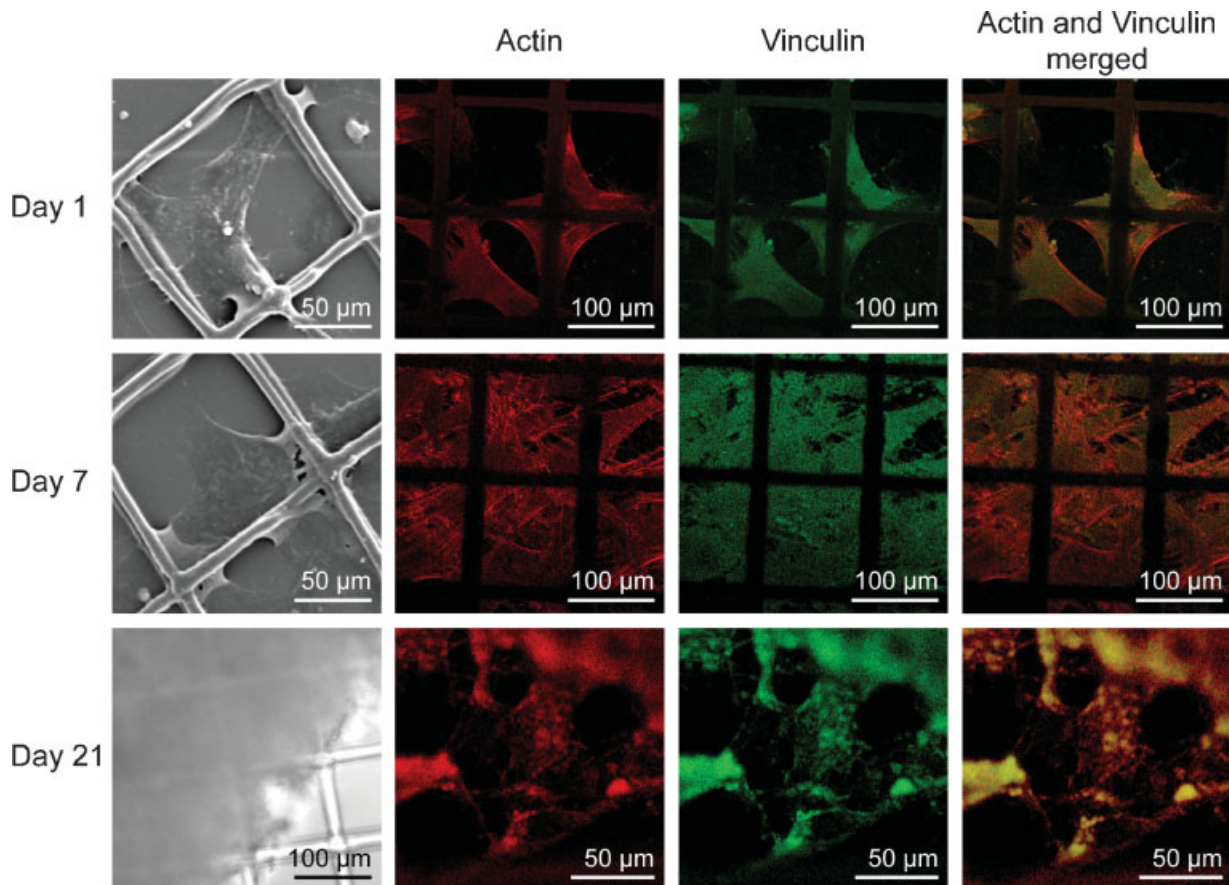
Figure 5. Morphological modulation of human bone marrow derived stem cells seeded on direct-write scaffold with Chondrogenic differentiation. Images show gradual overall change of cell morphology from spread to aggregated from Day 1 to Day 21. Immunoflurescent staining shows cytoskeletal proteins actin, vinculin, and an overlay of actin and vinculin.

Figure 6. Plot of glucosaminoglycan (GAG) accumulation normalized to DNA as a function of time for a silk fibroin direct-write scaffold and a cell pellet standard in the presence of chondrogenic soluble factors and a silk fibroin direct-write scaffold without chondrogenic media.

3. Conclusions

One important goal for tissue engineering is to produce patient-specific biological tissue substitutes that will match a specific defect. To repair large or complex tissue defects, custom-designed constructs with geometries fit to the specific defect site are desirable to improve integration. Our results provide an initial step toward the realization of microarchi-tectured designs based on 3D silk fibroin scaffolds that support the generation of 3D cartilaginous tissues. The behavior of hMSCs, as related to chondrogenic differentiation, demon-strated phenotypic outcomes supportive of their utility for this tissue type. Further, actin immunostaining showed changes from spread to punctuated morphology, indicative of temporal development of cartilaginous-like tissue. Also the amount of GAG normalized to DNA content increased with time of culture, further evidence for the utility of these protein scaffolds for tissue-specific outcomes. The development of controlled fibrous architectures has potential to help in the fundamental understanding of the role of architectural complexity on tissue development and remodelling, as well as the formation of multicellular aggregates for the complex

microenvironments of targeted tissue. By comparison with other methods for preparing 3D tissue engineering scaffolds from degradable polymeric systems, our approach confers important benefits such as, finer fiber diameter, avoidance of harsh processing conditions of temperature or toxic organic solvents, and the ability to precisely control complex architectures. Direct-write assembly offers a unique path forward in support of biomaterial scaffolding for human disease models, complex tissue interfaces and tissue gradients, all areas in need of new scaffold options where aqueous methods can be used to impart further functionalization.

4. Experimental

Silk Inks: Direct-write inks composed of 28–30 wt% aqueous silk fibroin solution were prepared by concentrating 8 wt% solution prepared as described previously [11,23]. In brief, cocoons of *B. mori* silkworm silk (Tajima Shoji Co., Ltd., Yokohama, Japan) were boiled for 30 min in an aqueous solution of 0.02 M Na_2CO_3, and then rinsed thoroughly with distilled water to extract the glue-like sericin proteins. The extracted fibroin was dissolved in 9.3M LiBr solution at 60 °C for 4 h, yielding a 20 wt% aqueous solution. This solution was dialyzed against distilled water using Slide-a-Lyzer dialysis cassettes (MWCO 3,500, Pierce) at room temperature for 3 days to remove the salt. The dialysate was centrifuged twice, each at −5 °C to 10 °C for 20 min, to remove impurities and aggregates. The solution obtained from this process was approximately 8 wt%. This silk fibroin aqueous solution (8 wt%, 9 mL) was then dialyzed against a 15 wt% poly(ethylene glycol) (PEG) (8000 g mol^{-1}, Sigma Aldrich) solution at room temperature by using Slide-a-Lyzer dialysis cassettes (MWCO 3500). The volume ratio of PEG solution to silk fibroin solution was 40:1. After approximately 14 h, the concentrated silk fibroin solution (28–30 wt%) was slowly removed by a syringe to avoid excessive shearing. All solutions were stored at 4 °C before use.

Direct-write assembly: Three-dimensional (3D) silk scaffolds were formed with micrometer-scale features using a three-axis micropositioning stage (ABL9000, Aerotech Inc., Pittsburgh, PA) controlled by customized software (3D Inks, Stillwater, OK). The concentrated silk fibroin solution was housed in a syringe (barrel diameter = 4.6 mm, EFD Inc., East Providence, RI) that was mounted on the *x-y-z* stage. The silk fibroin ink was extruded through a 5 μm tapered microcapillary nozzle that was pulled from a borosilicate glass tube (1.0 mm outer diameter and 0.58 mm inner diameter) using a P-2000 Laser Based Micropipette Puller (Sutter Instrument, Novato, CA) onto a stationary glass substrate. The silk ink was extruded under an applied pressure (800 Ultra dispensing system, EFD Inc.) of 20–70 kPa at a constant deposition speed of 2 mm s^{-1}. The ink was deposited into a coagulation reservoir (~200 μl) consisting of a methanol/(methanol + water) ratio of 0.86. As the ink exited the nozzle, a continuous rod-like filament formed that retained shape after rapid coagulation in the deposition reservoir. A reservoir composition of 86% methanol was deemed optimal, because it yielded a coagulated ink filament that was elastic enough to maintain shape while spanning unsupported regions of the structure, yet flexible enough to maintain flow through the deposition nozzle and adhere to the substrate and underlying layers. After patterning a 2D layer, the nozzle was incrementally raised in the *z*-direction to generate the next layer. This process was repeated until the desired 3D structure was formed. 3D periodic scaffolds composed of a simple tetragonal geometry were assembled by patterning an array of parallel (rod-like) filaments in the *x-y* plane such that their orientation was orthogonal to the previous layer. The center-to-center separation distance between filaments within a given layer was 100 μm and the overall scaffold dimensions were 2 mm × 2 mm with 2–6 layers.

The build time for each scaffold varied from 1 to 3 min, respectively. All structures were dried at ~22 °C and less than 35% relative humidity. After deposition, the crystallized fibers had a diameter of ~4.5 μm, based on SEM (S-4700 Scanning Electron Microscope, Hitachi Ltd., Tokyo, Japan).

Ink rheology: The rheological properties of silk fibroin solutions were determined using a controlled-stress rheometer (Bohlin CVO Rheometer, Malvern Instruments Ltd., Worcestershire, UK) fitted with a cone and plate geometry (CP 4/40, cone diameter of 40 mm with a 4° angle and gap width of 150 μm). The viscosity and shear rates of silk fibroin solutions of varying concentration (5–29 wt%) were acquired as a function of shear stress (τ) in a logarithmically ascending series of discrete steps. The elastic shear (G') and viscous (G'') moduli of a representative 29 wt% silk fibroin ink were measured using an oscillatory logarithmic stress sweep at a frequency of 1 Hz. Measurements were carried out at a temperature of 22 °C with a water solvent trap to reduce drying effects.

Fourier Transform Infrared (FTIR) Spectroscopy: The concentrated (~29 wt%) silk fibroin ink was printed directly on double polished silicon in a single layer pattern of 3 mm × 3 mm with a rod spacing of 20 μm through a 5 μm nozzle in a reservoir of 86% MeOH. The FTIR spectrum of the printed rods were compared to the spectrum from a dried film of concentrated silk fibroin. Measurements and analysis of the spectra and amide bands were performed with a Thermo Nicolet Nexus 670 FT-IR (Thermo Fisher Scientific, Inc., Waltham, MA).

AFM nanoindentation: Both direct-write and salt-leached [11] scaffolds were embedded in a medium grade epoxy resin (London Resin Company Ltd., England) and cured for at least 72 h at room temperature. Transverse and longitudinal specimens were prepared by sectioning the scaffolds embedded in resin using an ultramicrotome (RMC Scientific Corp., Tucson, AZ) with a diamond knife. No evidence of knife damage to the sample was observed. A Nanoscope IV, Dimension 3100 AFM (Digital Instruments, Santa Barbara, CA), was used in tapping mode with a RTESP single-beam silicon probe (Digital Instruments). The resonant frequency and force constant of the probe were 280–361 kHz and 30–40 N m^{-1}, respectively. A 22° compensation of the probe during the indentation was used to prevent the cantilever from plowing the surface laterally, typically along the *x* direction. Samples were prepared by sticking the sample on a flat metal disk with a thin layer of epoxy glue. Diffusion of the glue into the scaffold pore architecture can reinforce the structure. To avoid this problem, the epoxy glue was adhered first and cured for 5 min, almost to completion, before the scaffolds were placed on the material. The AFM indentation procedure consisted of three stages. First, the sample was inspected by AFM using tapping mode to locate the scaffold area for indentation, then the scan area was set to 0 nm. Next, the AFM was switched to force mode and the indentation performed. Finally, the AFM was switched back to tapping mode to image the indented area. All indentations were performed along the radial direction of the fiber. The elastic modulus of the silk architectures were evaluated using AFM nanoindentation [38,39].

Cell culture: For examination of cell growth and differentiation in vitro, 3D scaffolds were immersed in complete media (DMEM, 10% FCS, 100 mg mL^{-1} penicillin-streptomycin) for 4 h. hMSCs (50000 cells per scaffold, passage 2–3) were suspended in 20 μl DMEM, and seeded onto prewet scaffolds. Seeded scaffolds were incubated at 37 °C for 2 hrs to allow cell attachment. To keep the constructs hydrated, 10 μL DMEM was added every 15 min. Subsequently, 1 mL of chondrogenic medium was added per well. Chondrogenic medium was DMEM supplemented with penicillin-streptomycin, 100 nM dexamethasone, 50 mg mL^{-1} ascorbic acid-2-phosphate, insulin, transferrin, and selenious acid premix (6.25 mg mL^{-1} bovine insulin, 6.25 mg mL^{-1} transferrin, 6.25 mg mL^{-1} selenious acid, 5.33 mg mL^{-1} linoleic acid, 1.25 mg mL^{-1} bovine serum albumin). The medium was supplemented with 5 ng mL^{-1} FGF-2 and 10 ng mL^{-1} TGF-β1 for the first 4 days and then with only 10 ng mL^{-1} TGF-β1. The samples were cultured for up to 3 weeks at 37 °C and 5% CO_2 with medium changed twice weekly.

3D cell pellets were prepared in plastic culture plates following coating with a $50\,\mu g\,mL^{-1}$ poly-2-hydroxyethyl methacrylate (polyHEMA, Sigma, St. Louis, MO) solution to prevent cell binding. 50000 hMSCs per well were used [4].

Scanning Electron Microscopy: SEM images of 3D silk scaffolds were taken with a Hitachi S-4700 SEM (Hitachi Ltd., Tokyo, Japan). Prior to imaging, samples were coated with gold/palladium for 45 s (Emitech K575 Sputter Coater, Emitech Ltd., Ashford Kent, UK). Scaffolds seeded with hMSCs were fixed at different time points in PBS containing 2.5% glutaraldehyde for 1 hr at room temp, rinsed in PBS, and dehydrated in increasing concentrations of ethanol (25%, 50%, 60%, 80%, 100%) and air dried. After drying, they were sputter-coated with gold and viewed with a voltage of 10 kV under low vacuum.

Phase Contrast Microscopy and Staining of the Beta-Actin Cytoskeleton for Immunofluorescence: Cells were seeded on the silk scaffolds and kept in culture for up to 3 weeks. To visualize the cytoskeleton, the cells were rinsed in PBS, fixed with 4% paraformaldehyde in PBS for 30 min, permeabilized with 0.1% Triton-X100, and stained with anti-vinculin–FITC conjugate antibody and rhodamine-conjugated phalloidin (Sigma) for 30 min at 4 °C. The samples were investigated by a confocal laser scanning microscope (Leica, DMIRE2).

Biochemical Analysis: Pellets or tissue constructs were collected at each time point, washed with PBS, weighed and digested with proteinase K (1 mg mL^{-1} protease K in 50 mmol/L Tris with 1 mmol/L EDTA, 1 mmol/L iodoacetamide, and 10 μg mL^{-1} pepstatin-A) for 15 h at 56 °C. GAG content was measured spectrophotometrically using dimethylmethylene blue dye [49], with chondroitin sulfate as a standard. The GAG content was normalized to the amount of DNA, which was measured using a CyQUANT cell proliferation assay kit (Molecular Probes) with calf thymus DNA as a standard.

[1] C. Fischbach, R. Chen, T. Matsumoto, T. Schmelzle, J. S. Brugge, P. J. Polverini, D. J. Mooney, *Nat. Methods* **2007**, *4*, 855.

[2] S. Ghosh, D. L. Kaplan, *Advances in Tissue Engineering*, (Ed. L. Pollak) Imperial College Press, UK **2008**.

[3] M. Rosowski, M. Falb, M. Tschirschmann, R. Lauster, *Artif. Organs* **2006**, *30*, 775.

[4] S. Ghosh, G. C. Spagnoli, I. Martin, S. Ploegert, P. Demougin, M. Heberer, A. Reschner, *J. Cell. Physiol.* **2005**, *204*, 522.

[5] A. Birgersdotter, R. Sandberg, I. Ernberg, *Semin. in Cancer Biol.* **2005**, *15*, 405.

[6] B. Johnstone, T. M. Hering, A. I. Caplan, V. M. Goldberg, J. U. Yoo, *Exp. Cell. Res.* **1998**, *238*, 265.

[7] F. Barry, R. Boynton, B. Liu, J. Murphy, *Exp. Cell. Res.* **2001**, *268*, 189.

[8] A. A. Worster, B. D. Brower-Toland, L. A. Fortier, S. J. Bent, J. Williams, A. J. Nixon, *J. Orthop. Res.* **2001**, *19*, 738.

[9] D. R. Albrecht, G. H. Underhill, T. B. Wassermann, R. L. Sah, S. N. Bhatia, *Nat. Methods* **2006**, *3*, 369.

[10] L. E. Freed, F. Guilak, X. E. Guo, M. L. Gray, R. Tranquillo, J. W. Holmes, M. Radisic, M. V. Sefton, D. Kaplan, G. Vunjak-Novakovic, *Tissue Eng.* **2006**, *12*, 3285.

[11] S. Hofmann, H. Hagenmuller, A. M. Koch, R. Muller, G. Vunjak-Novakovic, D. L. Kaplan, H P Merkle, L. Meinel, *Biomaterials* **2007**, *28*, 1152.

[12] R. Nazarov, H. J. Jin, D L Kaplan, *Biomacromolecules* **2004**, *5*, 718.

[13] E. M. Sachs, J. S. Haggerty, M. J. Cima, U.S. Patent US5204055, 1993.

[14] S. Miot, T. Woodfield, A. U. Daniels, R. Suetterlin, I. Peterschmitt, M. Heberer, C. A. van Blitterswijk, J. Riesle, I. Martin, *Biomaterials* **2005**, *26*, 2479.

[15] D. W. Hutmacher, S. Cool, *J. Cell. Molec. Medicine* **2007**, *11*, 654.

[16] W. Yeong, C. Chua, K. Leong, M. Chandrasekaran, *Trends in Biotechnol.* **2004**, *22*, 643.

[17] D. W. Hutmacher, M. Sittinger, M. V. Risbud, *Trends in Biotechnol.* **2004**, *22*, 354.

[18] L. Moroni, J. R. de Wijn, C. A. van Blitterswijk, *Biomaterials.* **2006**, *27*, 974.

[19] A. Yousefi, C. Gauvin, L. Sun, R. W. DiRaddo, J. Fernandes, *Polym. Eng. Sci.* **2007**, *47*, 608.

[20] M. Zuwei, K. Masaya, I. Ryuji, S. Ramakrishna, *Tissue Eng.* **2005**, *11*, 101.

[21] G. M. Gratson, M. Zu, J. A. Lewis, *Nature 2004 428*, 386.

[22] J. A. Lewis, *Adv. Funct. Mater.* **2006**, *16*, 2193.

[23] X. Wang, X. Hu, A. Daley, O. Rabotyagova, P. Cebe, D. L. Kaplan, *J. Controlled Release* **2007**, *121*, 190.

[24] J. Nam, Y. H. Park, *J. Appl. Polym. Sci.* **2001**, *81*, 3008.

[25] D. Marolt, A. Augst, L. E. Freed, C. Vepari, R. Fajardo, N. Patel, M. Gray, M. Farley, D. L. Kaplan, G. Vunjak-Novakovic, *Biomaterials* **2006**, *27*, 6138.

[26] M. Lovett, C. Cannizzaro, L. Daheron, B. Messmer, G. Vunjak-Novakovic, D. L. Kaplan, *Biomaterials* **2007**, *28*, 5271.

[27] Y. Wang, H. J. Kim, G. Vunjak-Novakovic, D. L. Kaplan, *Biomaterials* **2006**, *27*, 6064.

[28] C. Vepari, D. L. Kaplan, *Prog. in Polym. Sci.* **2007**, *32*, 991.

[29] C. Li, C. Vepari, H. J. Jin, H. J. Kim, D. L. Kaplan, *Biomaterials* **2006**, *27*, 3115.

[30] H. Jin, S. V. Fridrikh, G. C. Rutledge, D. L. Kaplan, *Biomacromolecules* **2002**, *3*, 1233.

[31] X. Wang, J. A. Kluge, G. G. Leisk, D. L. Kaplan, *Biomaterials* **2008**, *29*, 1054.

[32] X. Chen, D. P. Knight, Z. Shao, F. Vollrath, *Polymer* **2001**, *42*, 9969.

[33] C. Holland, C. E. Terry, D. Porter, F. Vollrath, *Polymer* **2007**, *48*, 3388.

[34] H. J. Jin, D. L. Kaplan, *Nature* **2003**, *424*, 1057.

[35] T. Miyazawa, E. R. Blout, *J. Am. Chem. Soc.* **1961**, *83*, 712.

[36] Y. N. Chirgadz, B. V. Shestopa, S. V. Venyamin, *Biopolymers* **1973**, *12*, 1337.

[37] J. Magoshi, M. Mizuide, Y. Magoshi, K. Takahashi, M. Kubo, S. Nakamura, *J. Polym. Sci. B, Polym. Phys.* **1979**, *17*, 515.

[38] M. Wang, H. J. Jin, D. L. Kaplan, G. C. Rutledge, *Macromolecules* **2004**, *37*, 6856.

[39] E. P. S. Tan, C. T. Lim, *Composites Sci. Technol.* **2006**, *66*, 1102.

[40] N. C. Zanetti, M. Solursh, *J. Cell Biol.* **1984**, *99*, 115.

[41] P. D. Brown, P. Benya, *J. Cell Biol.* **1988**, *106*, 171.

[42] W. H. Goldmann, *Cell Biol. Int.* **2002**, *26*, 313.

[43] C. S. Chen, J. L. Alonso, E. Ostuni, G. M. Whitesides, D. E. Ingber, *Biochem. Biophys. Res. Commun.* **2003**, *307*, 355.

[44] A. Woods, G. Wang, F. Beier, *J. Biol. Chem.* **2005**, *280*, 11626.

[45] Y. B. Lim, S. S. Kang, W. G. An, Y. S. Lee, J. S. Chun, J. K. Sonn, *J. Cell. Biochem.* **2003**, *88*, 713.

[46] Y. Lim, S. Kang, T. K. Park, Y. Lee, *Biochem. Biophys. Res. Commun.* **2000**, *273*, 609.

[47] E. Langelier, R. Suetterlin, C. D. Hoemann, U. Aebi, M. D. Buschmann, *J. Histochem. Cytochem.* **2000**, *48*, 1307.

[48] S. P. Grogan, A. Barbero, J. Diaz-Romero, A. Cleton-Jansen, S. Soeder, R. Whiteside, P. C. W. Hogendoorn, J. Farhadi, T. Aigner, I. Martin, P. Mainil-Varlet, *Arthritis Rheum.* **2007**, *56*, 586.

[49] R. W. Farndale, D. J. Buttle, A. J. Barrett, *Biochim. Biophys. Acta.* **1986**, *883*, 173.